Acta Biomaterialia 9 (2013) 5447–5452

Contents lists available at SciVerse ScienceDirect

Acta Biomaterialia

journal homepage: www.elsevier.com/locate/actabiomat

Magnetic field activated lipid–polymer hybrid nanoparticles for stimuli-responsive drug release

Seong Deok Kong [a], Marta Sartor [a], Che-Ming Jack Hu [b], Weizhou Zhang [c], Liangfang Zhang [b,*], Sungho Jin [a,d,*]

[a] Materials Science and Engineering, University of California San Diego, La Jolla, CA 92093, USA
[b] Department of Nanoengineering, University of California San Diego, La Jolla, CA 92093, USA
[c] Department of Pharmacology, School of Medicine, University of California San Diego, La Jolla, CA 92093, USA
[d] Department of Mechanical and Aerospace Engineering, University of California San Diego, La Jolla, CA 92093, USA

ARTICLE INFO

Article history:
Received 25 July 2012
Received in revised form 31 October 2012
Accepted 5 November 2012
Available online 10 November 2012

Keywords:
Lipid–polymer hybrid nanoparticles
Magnetic beads
Drug delivery
Controlled drug release

ABSTRACT

Stimuli-responsive nanoparticles (SRNPs) offer the potential of enhancing the therapeutic efficacy and minimizing the side-effects of chemotherapeutics by controllably releasing the encapsulated drug at the target site. Currently controlled drug release through external activation remains a major challenge during the delivery of therapeutic agents. Here we report a lipid–polymer hybrid nanoparticle system containing magnetic beads for stimuli-responsive drug release using a remote radio frequency (RF) magnetic field. These hybrid nanoparticles show long-term stability in terms of particle size and polydispersity index in phosphate-buffered saline (PBS). Controllable loading of camptothecin (CPT) and Fe_3O_4 in the hybrid nanoparticles was demonstrated. RF-controlled drug release from these nanoparticles was observed. In addition, cellular uptake of the SRNPs into MT2 mouse breast cancer cells was examined. Using CPT as a model anticancer drug the nanoparticles showed a significant reduction in MT2 mouse breast cancer cell growth *in vitro* in the presence of a remote RF field. The ease of preparation, stability, and controllable drug release are the strengths of the platform and provide the opportunity to improve cancer chemotherapy.

1. Introduction

Nanotechnology for medical applications is an exciting and rapidly advancing field with a significant impact on diagnosis and therapeutics for the treatment of human diseases [1–7]. Nanoparticle-based drug delivery is of particular interest for cancer treatment, owing to such features as a prolonged circulation half-life, reduced non-specific uptake, and increased tumor accumulation through enhanced permeation and retention (EPR) or active targeting [8–10]. Currently over 20 nanoparticle-based therapeutics have been approved for clinical use and numerous products are under clinical testing [11–13]. Among these clinical or pre-clinical products liposomes and biodegradable polymeric nanoparticles are the most widely adopted carriers for drug delivery [14,15]. More recently lipid–polymer hybrid nanoparticles [16–20] have been developed by combining both liposomes and polymeric nanoparticles into a single delivery system. The resulting lipid–polymer hybrid nanostructure gives rise to unique advantages, such as ease of particle preparation, improved functionalizability, and more sustained drug release kinetics. These lipid–polymer hybrid nanoparticles have proven to be a robust platform in which different modalities can be incorporated for precision drug delivery [18].

The allure of on demand drug release, which promises enhanced therapeutic efficacy through targeted delivery, has motivated the development of stimuli-responsive delivery systems triggered by acidity, temperature, magnetic fields, and light irradiation [21–27]. Previously we presented a hollow silica nanocapsule capable of on–off switchable drug release via application of a remote radio frequency (RF) magnetic field [23]. Herein a one step nanoprecipitation process was used to prepare 80 nm lipid–polymer hybrid nanoparticles co-encapsulating 10 nm magnetic beads and a model anticancer drug, camptothecin (CPT). The nanocarrier platform possesses numerous advantages, including ease of preparation, sustained drug release, and excellent stability under physiological conditions [28,29]. The hydrophobic polymeric core of the platform readily encapsulated the water-insoluble drug for systemic delivery. The lipid coating provided a diffusional barrier that retards drug release in the absence of an external stimulus [28]. Upon RF magnetic field actuation localized heating by Fe_3O_4 inside the polymeric cores loosened the polymer matrices and accelerated drug release, resulting in increased cytotoxicity *in vitro* against a

* Corresponding authors. Tel.: +1 858 534 4903.
E-mail addresses: zhang@ucsd.edu (L. Zhang), jin@ucsd.edu (S. Jin).

1742-7061/$ - see front matter © 2012 Acta Materialia Inc. Published by Elsevier Ltd. All rights reserved.
http://dx.doi.org/10.1016/j.actbio.2012.11.006

mouse breast cancer cell line. Taking advantage of the robust lipid–polymer hybrid carrier platform we demonstrate the preparation of lipid–polymer hybrid nanoparticles for controlled drug release through a single step nanoprecipitation procedure, and also demonstrate stimuli-responsive drug release from such nanoparticles as well as their – cytotoxicity to cancer cells.

2. Materials and methods

2.1. General comments

All reagents were purchased from Sigma–Aldrich Inc. and Alfa Aesar, and used without further purification. The microscopic characterization of synthesized nanoparticles was carried out using a transmission electron microscope (FEI Tecnai G2 Sphera at 200 keV acceleration voltage). Various chemical and optical measurements were performed using a UV/vis spectrophotometer (Thermo BioMate3). To generate the RF magnetic field a Lepel LSS-2.5 RF power supply equipped with a water-cooled solenoid was used.

2.2. Synthesis of ~10 nm iron oxide nanoparticles

Monodisperse Fe_3O_4 nanoparticles were prepared according to a previous report [22]. Briefly, a mixture of 24 g $FeCl_3{\cdot}6H_2O$ and 9.82 g $FeCl_2{\cdot}4H_2O$ was reacted with 50 ml of ammonium hydroxide under nitrogen gas at 80 °C, and then the solution was allowed to react for 1.5 h after the addition of 3.76 g oleic acid. The prepared magnetite nanoparticles were washed with deionized water until the pH was neutral and subsequently transferred in situ into tetrahydrofuran (THF).

2.3. Synthesis of iron oxide-loaded lipid–polymer hybrid nanoparticles

Iron oxide-loaded lipid–polymer hybrid nanoparticles, herein designated stimuli-responsive nanoparticles (SRNPs), were prepared via self-assembly of poly(lactic-co-glycolic acid) (PLGA) having a glass transition temperature T_g of ~45 °C (Lactel, Pelham, AL) [30], refined soybean lecithin (molecular weight ~330 Da, Alfa Aesar, Ward Hill, MA), carboxyl-terminated 1,2-distearoyl-sn-glycero-3 phosphoethanolamine-N-carboxy(polyethylene glycol) (DSPE-PEG), and iron oxide nanoparticles through a single step nanoprecipitation method. Briefly, 0.12 mg lecithin and 0.26 mg DSPE-PEG were dissolved in 2 ml of 4 wt.% aqueous ethanol solution. The solution was heated to 68 °C to better disperse the lipid components. In parallel, 1 mg PLGA polymer and 400 μg iron oxide nanoparticles were dissolved in 1 ml of THF. The resulting PLGA solution was then dropwise added to the lipid solution under gentle stirring. The mixed solution was vortexed vigorously for 3 min, followed by gentle stirring for 3 h at room temperature. Following solvent evaporation the remaining organic solvent, free molecules, and unencapsulated iron oxide nanoparticles were removed by washing the SRNP solution three times using an Amicon Ultra-4 centrifugal filter (Millipore, Billerica, MA) with a molecular weight cut-off (MWCO) of 100 kDa. Removal of unencapsulated iron oxide nanoparticles (typically ~10 nm diameter) was verified through dynamic light scattering (DLS) measurements, which revealed a unimodal particle population 80 nm in diameter.

2.4. Characterization of stimuli-responsive nanoparticles

The SRNP size (diameter in nm) and polydispersity index (PDI) were measured by DLS using a Nano-ZS model ZEN3600 (Malvern, UK). The SRNPs (~500 μg) were dispersed in water (~1 ml) and the measurements were performed in triplicate at room temperature. The size and PDI of the SRNPs in water at room temperature were monitored for 30 days.

2.5. Measurement of CPT loading in stimuli-responsive nanoparticles

The SRNPs were prepared with different initial concentrations of CPT or iron oxide nanoparticles. To quantify the drug loading the SRNPs were dried and 1 ml of THF was added. The resulting solution was stirred for 3 h and subsequently filtered twice in 2 K MWCO Slide-A-Lyzer Cassettes (Millipore, Bellerica, MA) placed in an Eppendorf tube at 1500 r.p.m. for 5 min. Using non-CPT-loaded nanoparticles as the baseline control, the drug loading yield in the lipid–PLGA hybrid nanoparticles was quantified based on the absorbance at 362 nm as measured with a UV/vis spectrophotometer (Thermo BioMate3) following a previously published protocol [31].

2.6. Drug release characterization

For the drug release study 5 wt.% CPT-loaded SRNPs were prepared and then remote RF activated drug release was measured by UV/vis spectrophotometry. First, a 100 μl solution containing 5% CPT-loaded SRNPs was loaded on a 2K MWCO Slide-A-Lyzer filter. The filter was then inserted into a tube containing 1 ml deionized water. The resulting solution was exposed to RF (at 100 kHz) for 8 min twice, with a 4 min interval in between. A multiple RF exposure schedule was chosen so as to release a sufficient amount of drug with minimal risk of overheating and possible changes in the particle characteristics. The resulting drug concentration in the 1 ml solution was measured using UV/vis spectrophotometry and calibrated using a standard with predefined CPT concentrations. Following data collection the SRNP solution was placed in another tube containing 1 ml of fresh water. Cumulative CPT release was monitored at 37 °C for ~50 h. The study was performed in triplicate.

While our drug delivery experiments with tumor cells were performed in serum, our long-term storage stability studies were performed in PBS. A similar trend in stability is anticipated in serum-based solutions. In fact, we have already demonstrated that similar lipid–polymer hybrid nanoparticles (similar lipid and PLGA formulations, but without the magnetic nanoparticles embedded within the PLGA in the present work) remain stable in a serum environment over a relevant blood circulation period of 24 h [29].

2.7. Cellular internalization study

For the cellular internalization study 0.5 μg of a hydrophobic DiD dye was added to the solvent mixture containing 400 μg iron oxide nanoparticles prior to SRNP preparation following a previously published protocol [32]. The solvent mixture was added dropwise to an aqueous mixture of lecithin and DSPE-PEG. Following 3 h solvent evaporation the particles were washed in Amicon filters prior to use. The murine breast cancer cell line MT2 was maintained in Dulbecco's modified Eagle's medium (Gibco-BRL, Grand Island, NY) supplemented with 10% fetal calf serum (FCS) (Hyclone, Logan, UT), penicillin/streptomycin (Gibco-BRL), L-glutamine (Gibco-BRL), MEM non-essential amino acids (GibcoBRL), sodium bicarbonate (Cellgro, Herndon, VA), and sodium pyruvate (Gibco-BRL). The cells were cultured at 37 °C with 5% CO_2 and plated in chamber slides (Cab-Tek II, eight wells, Nunc, Rochester, NY) with the aforementioned medium. On the day of the experiment MT2 cells were washed with prewarmed PBS and incubated with prewarmed medium for 30 min before adding 100 μg Fe_3O_4-loaded nanoparticles stained with DiD dyes. The nanoparticles were incubated with the cells for 40 min at 37 °C, washed three times with PBS, fixed with tissue fixative (Millipore, Bellerica, MA) for 15 min at room temperature and stained with 4′,6-diamidino-2-phenylindole (DAPI) (nuclear staining). The cells were then

permeabilized in 0.1% Triton X-100 in PBS for 1 min, actin stained with FITC-conjugated phalloidin (Invitrogen) for 15 min, mounted in ProLong Gold antifade reagent (Invitrogen), and imaged using deconvolution scanning fluorescence microscopy (DeltaVision System, Applied Precision, Issaquah, WA). Digital images of blue, green, and red fluorescence were acquired using a 20× objective and DAPI (excitation/emission 350/470 nm), FITC (excitation/emission 490/525 nm), and CY5 (excitation/emission 640/670 nm) filters, respectively. Images were overlaid using softWoRx software.

2.8. In vitro cell viability test

The cells for the in vitro experiments were MT2 mouse mammary tumor cells derived from MMTV-c-Neu Tg mice from Dr. Michael Karin's laboratory (University of California, San Diego, CA). MT2 cells were maintained in F12 medium (Invitrogen) supplemented with 10% fetal bovine serum, 10 ng ml^{-1} EGF, 5 μg ml^{-1} of insulin, 1 μg ml^{-1} hydrocortisone, 100 U ml^{-1} penicillin, and 100 μg ml^{-1} streptomycin. All cells were cultured at 37 °C in a 5% CO_2, 95% air humidified atmosphere. Initially 1×10^5 MT2 mouse melanoma cells were seeded into three plates (35 × 10 mm tissue culture plates) in 2 ml of complete medium and incubated overnight. The solutions exposed vs. not exposed to RF were prepared with 1.2 ml of PBS and 600 μl of SRNP solution which was loaded on an Amicon Ultra-4 centrifugal filter (Millipore, Billerica, MA) with a MWCO of 100 kDa. The cell culture plates were placed inside the solenoid coil during RF activation. Drug release was performed by two 15 min RF exposures with a 5 min holding period between the exposures (total run time 40 min), which was designated "W/RF". The "W/O RF" experiments (no RF field applied to the SRNPs) were run for an equal total time of 40 min. The cells were washed and incubated in fresh medium. The cells in the experimental groups without RF activation were incubated with the particle mixtures for 40 min, washed, and cultured in 2 ml of fresh medium. After 48 h incubation MTT assays (Promega) were performed following the manufacturer's instructions to determine the viability of the cells. The cell viability data is plotted as bar graphs. The averages ± standard error bars are included in the bar graph plots. *P* values after performing ANOVA (Student–Newman–Keuls method) reaching a statistical significance of $P < 0.05$ are marked on the graphs. The study was performed in triplicate.

3. Results and discussion

3.1. Characterization of stimuli-responsive nanoparticles

Fig. 1a shows a schematic representation of the lipid–polymer hybrid nanoparticles. Magnetic nanoparticles and CPT were co-encapsulated in a PLGA matrix, which is stabilized by a monolayer of phospholipids and lipid–PEG conjugates. The hybrid nanoparticles are 80 nm spheres containing several 10 nm superparamagnetic Fe_3O_4 magnetite beads. To synthesize the SRNPs the iron oxide particle loading was first confirmed using transmission electron microscopy (TEM) in the absence of uranyl acetate staining. In order to visualize the completed SRNPs by TEM (Figs. 1b and S1) we used uranyl acetate staining. This stain contains a heavy metal which remains on the outer surface of the SRNPs and blocks TEM imaging of the iron oxide particles within the PLGA matrix. However, occasionally some of the lipid particles were only partially stained with uranyl acetate, and in such cases iron oxide nanoparticles were observed in the TEM images. The long-term stability of the lipid–PLGA hybrid nanoparticles loaded with Fe_3O_4 particles was examined by monitoring the particle size and PDI in PBS over time. As shown in Fig. 2, DLS measurements showed no significant change in average particle size or PDI during the observation period, suggesting that the hybrid particle formulation could be stored for long periods of time. The particles remained at around 80 nm with a PDI of 0.13 over the course of 30 days. Given that the PLGA used for SRNP preparation (50:50 PLA:PGA, $M_W \approx 100$ kDa) had an approximate half-life of 3 weeks, the particles probably became increasingly porous over time [33]. However, coating the particle surface with a lipid monolayer may reduce water penetration rate into the polymer core and thus reduce the PLGA degradation rate [20]. The effect of the increasing porosity on the stimuli-responsive drug release profile of the SRNPs remains to be investigated.

3.2. CPT drug loading in the stimuli-responsive nanoparticles

We next demonstrated that different concentrations of CPT can be loaded into the SRNPs (Fig. 3a). Controllable CPT loading from 1 to 10 wt.% is shown in Fig. 3a. We further showed that the number of Fe_3O_4 magnetic nanoparticles can be altered while maintaining the same amount of CPT in the lipid–PLGA hybrid nanoparticles (Fig. 3b).

3.3. RF activated drug release

The release of CPT from the SRNPs was activated by an applied RF field (at 100 kHz). Fig. 4 shows the cumulative CPT release profile from the hybrid nanoparticles. After 46 h monitoring of drug release from the SRNPs CPT was no longer detectable by UV/vis spectroscopy, so this accumulated amount was taken as representing approximately 100% CPT release and the other data points were normalized accordingly. A dramatic increase in the amount of released drug, approximately one order of magnitude higher,

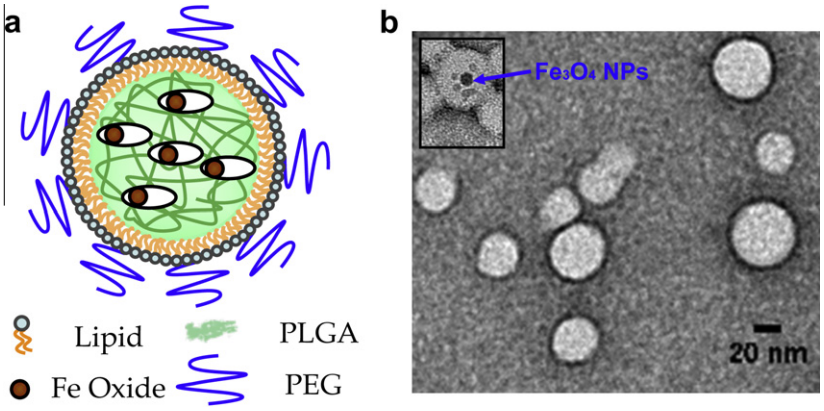

Fig. 1. Synthesis of lipid–PLGA hybrid nanoparticles as a drug carrier. (a) Schematic representation showing PLGA nanoparticles with embedded iron oxide nanoparticles and a lipid monolayer shell. (b) TEM micrograph of spherical lipid–PLGA hybrid nanoparticles. (Inset) Magnetic nanoparticles trapped in the lipid–PLGA hybrid nanoparticles.

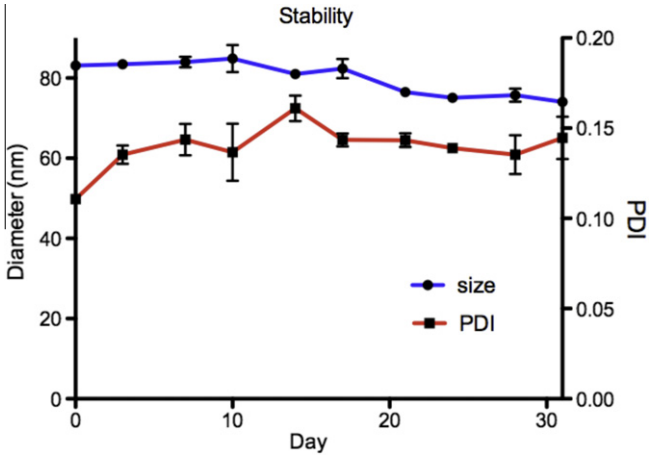

Fig. 2. Long-term stability of the lipid–PLGA hybrid nanoparticles containing 40 wt.% Fe_3O_4 nanoparticles in PBS at room temperature, which was monitored for up to 1 month.

occurred when the RF magnetic field was applied. The increased drug release can be attributed to local heating in the polymeric matrix by the magnetic particles upon RF magnetic field actuation. The extent of such remotely triggered heating of magnetic nanoparticles was previously demonstrated to correlate directly with the number of Fe_3O_4 nanoparticles as well as the duration of the applied RF magnetic field [23]. Owing to the relatively low glass transition temperature of PLGA (~45 °C) a temperature rise in the PLGA matrix can loosen the polymer mesh and cause the loaded CPT to more easily diffuse out. With both Fe_3O_4 loading and RF activation 60% cumulative drug release was observed in 5 h. When the iron oxide particles and/or the magnetic field activation were missing the cumulative CPT release remained unchanged at approximately 10% at the 5 h mark. The results indicate that the iron oxide loading alone has a minimal effect on CPT drug release and field activation was necessary to accelerate CPT release.

Compared with previously reported magnetically triggerable SRNPs, for example as reported in Kong et al. [23], the lipid–polymer hybrid SRNPs in the present work enable a comparable amount of CPT release, ~7 μg CPT per mg nanocapsules (CPT molecular weight ≈ 350 g mol^{-1}). However, the present SRNPs with lipid and PLGA components are more biocompatible due to the biodegradability of the materials involved.

3.4. Cellular uptake and in vitro cytotoxicity

Cellular uptake of the SRNPs into MT2 mouse breast cancer cells was examined. 100 μl of fluorescent SRNPs were incubated with the MT2 cells for 1 h and subsequently imaged using deconvolution scanning fluorescence microscopy. Fig. 5 shows internalization of the fluorescent particles by the MT2 cells. As DiD dye has been previously shown to exhibit minimal release from PLGA nanoparticles [32], and as the fluorescence of DiD within the cells appeared as distinct particles, it can be logically inferred that the observed red fluorescence corresponds to endocytosed SRNPs.

In order to validate magnetic field-driven drug release from the SRNPs we examined the in vitro viability of MT2 mouse breast cancer cells in the presence of SRNPs containing CPT. Fig. 6 shows the relative viability of MT2 mouse breast cancer cells in the presence of various nanoparticle samples. The first bar represents the control sample with no nanoparticles present, while the second bar represents the CPT-free nanoparticles without field activation. The third bar represents the CPT-free nanoparticles upon field activation, which shows a similar MT2 growth rate as the control. The fifth bar shows that the CPT-loaded nanoparticles triggered by a RF magnetic field resulted in significantly suppressed cancer cell growth, while the fourth bar, for non-activated particles, shows a similar cell growth to the control. Clearly, the CPT-loaded SRNPs under RF exposure stimulating the "on demand" release had noticeable and desirable effects on cell viability. Collectively these results indicate that CPT-free Fe_3O_4-loaded particles have no significant toxicity to tumor cells in the presence or absence of RF activation. However, the CPT-filled particles resulted in a dramatic reduction in tumor cell viability upon RF activation. The cytotoxicity results are consistent with the drug release study (Fig. 4), in which RF exposure substantially increased drug release from the Fe_3O_4-loaded lipid–PLGA hybrid nanoparticles. This accelerated drug release probably increased the effective cellular concentration of CPT and resulted in enhanced cytotoxicity. Compared with previously reported SRNP systems examined under similar conditions [23], the lipid–polymer nanoparticle platform examined in the current study showed similar or better tumor cell growth inhibition of MT2 cells.

As the cytotoxicity of drug delivery capsules is an important issue it will be worthwhile to perform a more thorough study of toxicity as a function of the magnetic nanoparticle concentration and drug release procedure. The size of the SRNP nanocapsules as well as the type of biodegradable polymer can also be altered and optimized for enhanced drug release behavior and controlled

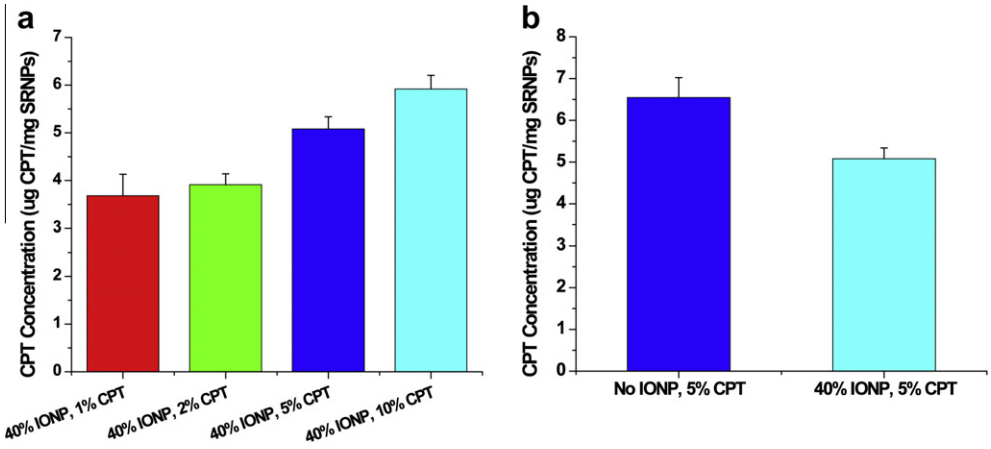

Fig. 3. Controlled drug loading in lipid–PLGA hybrid nanoparticles. (a) CPT loading was varied by using different initial concentrations of CPT. (b) CPT loading was not affected by the embedded magnetic nanoparticles in the hybrid nanoparticles.

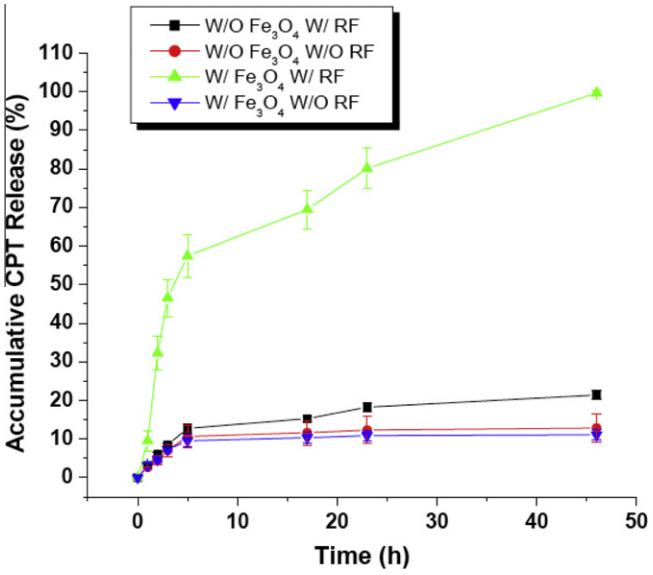

Fig. 4. Controlled drug release from CPT-containing lipid–PLGA hybrid nanoparticles in a RF magnetic field. Remote magnetic field heating of the PLGA matrix containing magnetic nanoparticles stimulated rapid drug release. The cumulative amount of CPT released was monitored for ~50 h. Particles were exposed to RF twice for 4 min each with a break between exposures.

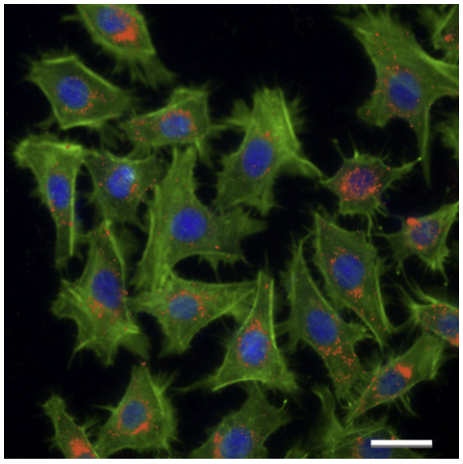

Fig. 5. Fluorescence microscopy image demonstrating cellular internalization of the Fe_3O_4-loaded nanoparticles (visualized with red DiD dyes in MT2 mouse breast cancer cells (blue DAPI nuclear staining, green phalloidin actin staining). Scale bar 20 μm.

cytotoxicity. Such studies towards more optimized nanoparticle concentrations and capsule structures will be conducted and the results will be reported in future publications.

Additional studies of magnetically stimulated controlled release of other types of anticancer drugs or different drugs for other therapeutics applications would also be interesting. Since there are magnetic particles present within the SRNP capsules a study of possible blood–brain barrier (BBB) crossing utilizing a direct current magnetic vector followed by RF magnetic field stimulated drug release may also be worthwhile.

4. Conclusion

We have successfully synthesized lipid–PLGA hybrid nanoparticles containing magnetic nanoparticles and demonstrated stimuli-responsive controlled drug release by application of a remote RF field. The long-term stability of these hybrid nanoparticles in terms of particle size and polydispersity index were confirmed in PBS. The CPT and Fe_3O_4 loadings were controllable. In vitro cytotoxicity results indicate that these hybrid nanoparticles can be made more effective against tumor cells by RF activation. Such remote controllable drug nanocarriers may provide advanced drug delivery technologies for multiple therapeutic purposes.

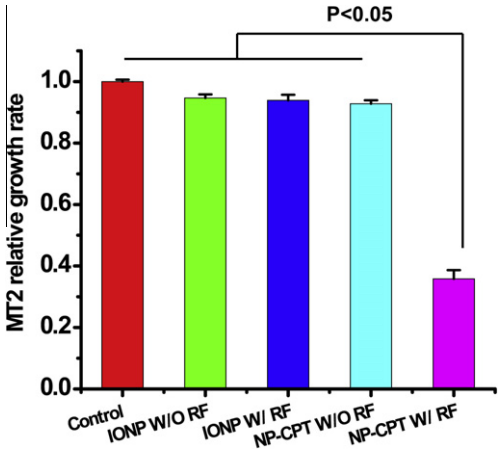

Fig. 6. Comparative growth rates (MTT assay) of MT2 mouse breast cancer cells treated with CPT-free and CPT-filled Fe_3O_4-loaded lipid–PLGA hybrid nanoparticles in the presence and absence of RF field activation.

Acknowledgements

We acknowledge financial support by the Iwama Fund at the University of California San Diego and the NSF through Grants DMR-1006081 (S.J.) and CMMI-1031239 (L.Z.).

Appendix A. Figures with essential colour discrimination

Certain figures in this article, particularly Figs. 1–6, are difficult to interpret in black and white. The full colour images can be found in the on-line version, at http://dx.doi.org/10.1016/j.actbio.2012.11.006.

Appendix B. Supplementary data

Supplementary data associated with this article can be found, in the online version, at http://dx.doi.org/10.1016/j.actbio.2012.11.006.

References

[1] Beduneau A, Saulnier P, Benoit JP. Active targeting of brain tumors using nanocarriers. Biomaterials 2007;28:4947–67.
[2] Brannon-Peppas L, Blanchette JO. Nanoparticle and targeted systems for cancer therapy. Adv Drug Deliv Rev 2004;56:1649–59.
[3] Cuenca AG, Jiang H, Hochwald SN, Delano M, Cance WG, Grobmyer SR. Emerging implications of nanotechnology on cancer diagnostics and therapeutics. Cancer 2006;107:459–66.
[4] Farokhzad OC, Langer R. Nanomedicine: developing smarter therapeutic and diagnostic modalities. Adv Drug Deliv Rev 2006;58:1456–9.
[5] Groneberg DA, Giersig M, Welte T, Pison U. Nanoparticle-based diagnosis and therapy. Curr Drug Targets 2006;7:643–8.
[6] Jin S, Ye KM. Nanoparticle-mediated drug delivery and gene therapy. Biotechnol Prog 2007;23:32–41.
[7] Sonvico F, Dubernet C, Colombo P, Couvreur P. Metallic colloid nanotechnology, applications in diagnosis and therapeutics. Curr Pharm Des 2005;11:2091–105.
[8] Couvreur P, Vauthier C. Nanotechnology: intelligent design to treat complex disease. Pharm Res 2006;23:1417–50.
[9] Hobbs SK, Monsky WL, Yuan F, Roberts WG, Griffith L, Torchilin VP, et al. Regulation of transport pathways in tumor vessels: role of tumor type and microenvironment. Proc Natl Acad Sci USA 1998;95:4607–12.

[10] Wang AZ, Gu F, Zhang LF, Chan JM, Radovic-Moreno A, Shaikh MR, et al. Biofunctionalized targeted nanoparticles for therapeutic applications. Expert Opin Biol Ther 2008;8:1063–70.
[11] Davis ME, Chen Z, Shin DM. Nanoparticle therapeutics: an emerging treatment modality for cancer. Nat Rev Drug Discov 2008;7:771–82.
[12] Wagner V, Dullaart A, Bock AK, Zweck A. The emerging nanomedicine landscape. Nat Biotechnol 2006;24:1211–7.
[13] Zhang L, Gu FX, Chan JM, Wang AZ, Langer RS, Farokhzad OC. Nanoparticles in medicine: therapeutic applications and developments. Clin Pharm Ther 2008;83:761–9.
[14] Abra RM, Bankert RB, Chen F, Egilmez NK, Huang K, Saville R, et al. The next generation of liposome delivery systems: recent experience with tumor-targeted, sterically-stabilized immunoliposomes and active-loading gradients. J Liposome Res 2002;12:1–3.
[15] Cheng J, Teply BA, Sherifi I, Sung J, Luther G, Gu FX, et al. Formulation of functionalized PLGA–PEG nanoparticles for in vivo targeted drug delivery. Biomaterials 2007;28:869–76.
[16] Chan JM, Zhang LF, Tong R, Ghosh D, Gao WW, Liao G, et al. Spatiotemporal controlled delivery of nanoparticles to injured vasculature. Proc Natl Acad Sci USA 2010;107:2213–8.
[17] Chan JM, Zhang LF, Yuet KP, Liao G, Rhee JW, Langer R, et al. PLGA–lecithin–PEG core–shell nanoparticles for controlled drug delivery. Biomaterials 2009;30:1627–34.
[18] Fang RH, Aryal S, Hu CMJ, Zhang LF. Quick synthesis of lipid–polymer hybrid nanoparticles with low polydispersity using a single-step sonication method. Langmuir 2010;26:16958–62.
[19] Liu YT, Li K, Pan J, Liu B, Feng SS. Folic acid conjugated nanoparticles of mixed lipid monolayer shell and biodegradable polymer core for targeted delivery of Docetaxel. Biomaterials 2010;31:330–8.
[20] Zhang L, Chan JM, Gu FX, Rhee J-W, Wang AZ, Radovic-Moreno AF, et al. Self-assembled lipid–polymer hybrid nanoparticles: a robust drug delivery platform. ACS Nano 2008;2:1696–702.
[21] Kaneko Y, Nakamura S, Sakai K, Kikuchi A, Aoyagi T, Sakurai Y, et al. Deswelling mechanism for comb-type grafted poly(N-isopropylacrylamnide) hydrogels with rapid temperature responses. Polym Gels Netw 1998;6:333–45.
[22] Kong SD, Luong A, Manorek G, Howell SB, Yang J. Acidic hydrolysis of N-ethoxybenzylimidazoles (NEBIs): potential applications as pH-sensitive linkers for drug delivery. Bioconjug Chem 2007;18:293–6.
[23] Kong SD, Zhang WZ, Lee JH, Brammer K, Lal R, Karin M, et al. Magnetically vectored nanocapsules for tumor penetration and remotely switchable on-demand drug release. Nano Lett 2010;10:5088–92.
[24] Kost J, Wolfrum J, Langer R. Magnetically enhanced insulin release in diabetic rats. J Biomed Mater Res 1987;21:1367–73.
[25] Luong A, Issarapanichkit T, Kong SD, Fong R, Yang J. pH-sensitive, N-ethoxybenzylimidazole (NEBI) bifunctional crosslinkers enable triggered release of therapeutics from drug delivery carriers. Org Biomol Chem 2010;8:5105–9.
[26] Sawahata K, Hara M, Yasunaga H, Osada Y. Electrically controlled drug delivery system using polyelectrolyte gels. J Control Release 1990;14:253–62.
[27] Shimoboji T, Larenas E, Fowler T, Kulkarni S, Hoffman AS, Stayton PS. Photoresponsive polymer–enzyme switches. Proc Natl Acad Sci USA 2002;99:16592–6.
[28] Zhang L, Chan J, Gu F, Rhee J-W, Wang A, Radovic-Moreno A, et al. Self-assembled lipid–polymer hybrid nanoparticles: a robust drug delivery platform. ACS Nano 2008;2:1696–702.
[29] Fang RH, Aryal S, Hu C-M, Zhang L. Quick synthesis of lipid–polymer hybrid nanoparticles with low polydispersity using a single-step sonication method. Langmuir 2010;26:16958–62.
[30] Muthu MS. Nanoparticles based on PLGA and its co-polymer: an overview. Asian J Pharm 2009;3:266–73.
[31] Aryal S, Hu CM, Zhang L. Polymeric nanoparticles with precise ratiometric control over drug loading for combination therapy. Mol Pharmacol 2011;8:1401–7.
[32] Hu CM, Zhang L, Aryal S, Cheung C, Fang RH, Zhang L. Erythrocyte membrane-camouflaged polymeric nanoparticles as a biomimetic delivery platform. Proc Natl Acad Sci USA 2011;108:10980–5.
[33] Lu L, Peter SJ, Lyman MD, Lai HL, Leite SM, Tamada JA, et al. In vitro and in vivo degradation of porous poly(DL-lactic-co-glycolic acid) foams. Biomaterials 2000;21:1837–45.